Chemical Science

ROYAL SOCIETY OF CHEMISTRY

EDGE ARTICLE

View Article Online
View Journal | View Issue

Cite this: *Chem. Sci.*, 2025, **16**, 16259

All publication charges for this article have been paid for by the Royal Society of Chemistry

Received 11th May 2025
Accepted 4th August 2025

DOI: 10.1039/d5sc03403e

rsc.li/chemical-science

Multi-electron redox reactivity of a thorium(II) hydride synthon

Xianghui Shi, †[a] Guorui Qin, †[a] Peng Deng, [ab] Iker Del Rosal, [c] Laurent Maron *[c] and Jianhua Cheng *[ab]

Molecular thorium complexes are dominated by stable tetravalent thorium, while subvalent thorium and the relevant synthons are very limited. Herein, we report that hydrogenolysis of the half-sandwich pentaarylcyclopentadienyl-supported thorium tribenzyl complex $[(Cp^{Ar5})Th(p\text{-}CH_2\text{–}C_6H_4\text{–}Me)_3]$ (**1**) (Cp^{Ar5} = C_5Ar_5, Ar = 3,5-$^{i}Pr_2$–C_6H_3) affords the double-sandwich bimetallic hydride complex $[(Cp^{Ar5})Th(\mu\text{-}H)]_2$ (**2**), in which one of the five aryl groups in the Cp^{Ar5} ligand is selectively reduced to a puckered di-anionic 1,4-cyclohexadienyl. Complex **2** can be regarded as a thorium(II) hydride synthon, and exhibits unique redox-active reactivity towards various substrates. Complex **2** not only serves as the six-electron transfer reagent in the reduction of Te and N_3SiMe_3, leading to the formation of $[(Cp^{Ar5})Th(THF)]_2(\mu\text{-}Te)_3$ (**3**) and $[(Cp^{Ar5})Th(\mu\text{-}N_3)(\mu\text{-}NSiMe_3)]_2$ (**4**), but also promotes the four-electron reductive coupling of CS_2 and benzonitrile accompanied by Th–H addition, resulting in the isolation of $[(Cp^{Ar5})Th(\mu\text{-}\eta^2\text{:}\eta^2\text{-}CS_3)(\mu\text{-}S)(\mu\text{-}\eta^4\text{:}\eta^1\text{-}SCH{=}CHS)Th(Cp^{Ar5})]$ (**5**) and $[(Cp^{Ar5})Th(PhCN)_2(\mu\text{-}NCH_2Ph)\{\eta^1,\kappa^3\text{-}NC(Ph){=}C(Ph)NC(Ph){=}NC(Ph){=}N\}Th(Cp^{Ar5})]$ (**6**) respectively.

Introduction

Compared with the rich redox chemistry of uranium, that of thorium is rather limited.[1] Thorium complexes predominantly exist in the +4 oxidation state due to their high stability, while accessing lower oxidation states, such as Th(II)[2] and Th(III)[3] complexes, remains highly challenging. In turn, actinide complexes featuring the reduced arene ligands continue to receive intense interest, as they are of fundamental importance in understanding the bonding nature and extent of covalency between the f-block metal and organometallic ligands, and they are also regarded as potential multi-electron reductants. The thorium(IV)arene complexes were typically synthesized using strong reducing agents (mostly alkaline metals).[4] Examples include $[\{(Et_8\text{-calix[4]tetrapyrrole})Th\}\{K(DME)\}(\eta^4\text{-}C_{10}H_8)]^-$,[4b] $[Th((OSiR_2Ar)_3\text{-arene})(THF)_2]^-$ (R = O^{t}Bu, Ph),[4c] $[K(OSi(O^tBu)_3)_3Th]_x(C_{10}H_8)]$ (x = 1 or 2)[4d] and $[(NN^{TBS})Th(THF)]_2(\mu\text{-}\eta^6,\eta^6\text{-arene})$ (NN^{TBS} = fc-(NSi^{t}BuMe$_2$)$_2$, fc = 1,1′-ferrocenediyl),[4e] which can facilitate multi-electron reductive reactions with a variety of substrates, thus acting as Th(II) synthons (Fig. 1).

The synthesis, structure and reactivity of actinide hydride complexes have occupied a central place in the organometallic chemistry of these elements, due to their important role in varied organic transformations and polymerizations.[5] Recently, our group disclosed the first examples of thorium trihydrido complexes supported by alkyl-substituted cyclopentadienyl ligands $[(Cp^{Me4R})Th(\mu\text{-}H)_3]_n$ (R = H, n = 8; R = Me, n = 7; R = SiMe$_3$, n = 6).[6] The nuclearity of metal clusters declines as the steric bulk of the cyclopentadienyl ligand increases (Scheme 1). Inspired by this rule, we decided to embark on the synthesis of low-nuclear thorium trihydrido species, such as dimeric ones.

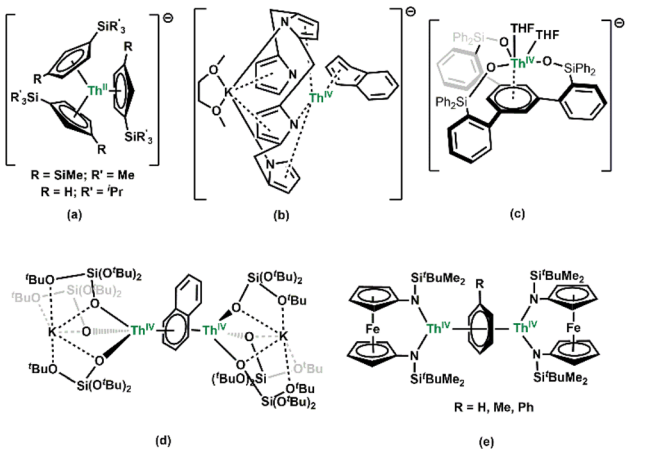

Fig. 1 Th(II) complexes (a) and selected thorium arene/arenide complexes (b–e).

[a]*State Key Laboratory of Polymer Science and Technology, Changchun Institute of Applied Chemistry, Chinese Academy of Sciences, No. 5625, Renmin Street, Changchun 130022, China. E-mail: jhcheng@ciac.ac.cn*

[b]*School of Applied Chemistry and Engineering, University of Science and Technology of China, Hefei, Anhui, 230026, China*

[c]*LPCNO, CNRS, INSA, UPS, Université de Toulouse, 135 Avenue de Rangueil, 31077 Toulouse, France. E-mail: laurent.maron@irsamc.ups-tlse.fr*

† X. S. and G. Q. contributed equally.

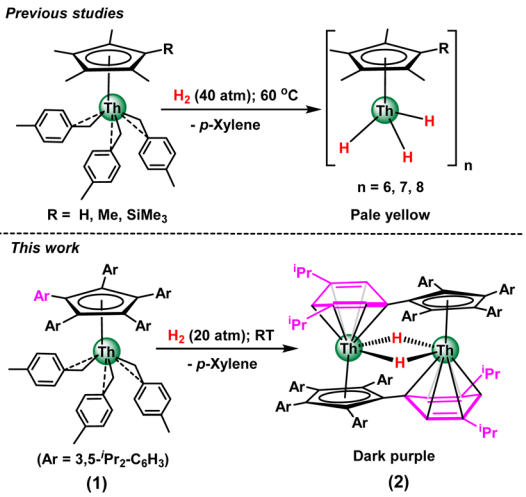

Scheme 1 Hydrogenolysis of mono-Cp ligated thorium tri-benzyl complexes.

The penta-arylcyclopentadienyl ligand is generally considered to be redox inactive and has been widely used as a monoanionic ancillary ligand across the periodic table.[7] Also recently, the super-bulky penta-arylcyclopentadienyl ligand (Cp^{Ar*5} = C_5Ar_5, Ar = 3,5-^{t}Bu$_2$–C$_6$H$_3$) was introduced to stabilize the mononuclear thorium dihydrido complex [(Cp^{Ar*5})(Cp*)ThH$_2$(THF)], with the combination of Cp* (Cp* = C_5Me_5) ligands.[8] However, the hydrogenolysis reaction of [(Cp^{Ar*5})Th(*p*-CH$_2$–C$_6$H$_4$–Me)$_3$] with H_2 in hexane seemed very complicated, and no characterizable product was obtained. Considering the steric effect as a crucial factor, we turned our attention to the slightly less bulky penta-arylcyclopentadienyl ligand Cp^{Ar5} (C_5Ar_5, Ar = 3,5-^{i}Pr$_2$–C$_6$H$_3$).[9] In sharp contrast to the previous hydrogenolysis reactions of alkyl-substituted cyclopentadienyl (Cp^{Me4R}) ligated thorium tribenzyl complexes [(Cp^{Me4R})Th(*p*-CH$_2$–C$_6$H$_4$–Me)$_3$] (R = H, Me, SiMe$_3$), which yielded multi-nuclear thorium trihydrido clusters [(Cp^{Me4R})Th(μ-H)$_3$]$_n$ as a pale-yellow solid,[6] moderate-pressure hydrogenolysis of [(Cp^{Ar5})Th(*p*-CH$_2$–C$_6$H$_4$–Me)$_3$] (**1**) with H_2 at 20 atm in hexane successfully led to the formation of the first example of double-sandwich bimetallic thorium hydride complex [(Cp^{Ar5})Th(μ-H)]$_2$ (**2**) stabilized by the tri-anionic penta-arylcyclopentadienyl ligands as a dark-purple solid in 82% isolated yield (Scheme 1). The redox reactivities of complex **2** with tellurium (Te), trimethylsilyl azide (N_3SiMe_3), carbon disulfide (CS_2) and benzonitrile (PhCN), which involve the multi-electron transfer process, are presented as well.

Results and discussion

The ^{1}H NMR spectra of [(Cp^{Ar5})Th(μ-H)]$_2$ (**2**) in C_6D_6 show the bridging hydride signal at 5.85 ppm, which is further corroborated by the deuterated analogue [(Cp^{Ar5})Th(μ-D)]$_2$ (**2-D**) (Fig. S8). Notably, the hydride chemical shift in complex **2** is at extraordinarily higher field than those in the previously reported molecular thorium trihydrido complexes [(Cp^{Me4R})Th(μ-H)$_3$]$_n$ (16.68–16.44 ppm),[6] thorium dihydrido complexes [(Cp*)$_2$ThH$_2$]$_2$ (19.25 ppm),[10b] [(Cp^{Ar*5})(Cp*)ThH$_2$(THF)] (23.47 ppm)[8] and [(2,6-^{t}Bu$_2$–C$_6$H$_3$O)$_2$Th(μ-H)$_2$]$_3$ (20.54 ppm),[10i] as well as thorium monohydrido complexes [(Cp^{Me4})$_3$ThH] (15.34 ppm)[10c] and [(Cp*)$_3$ThH] (15.40 ppm).[10h] Additionally, the five aryl groups in complex **2** exhibited relatively rigid behavior in d_8-toluene at varying temperatures (Fig. S9), in contrast to the fluxional nature of complex **1**.

Hydrogenolysis of complex **1** in aromatic solvents (toluene or benzene) afforded complex **2** with a relatively low isolated yield of 60%. When the hydrogenolysis reactions were carried out in donor solvents, such as THF, no formation of complex **2** was observed. Furthermore, ^{1}H NMR spectroscopic studies revealed that complex **2** remained stable in the presence of toluene or benzene at 80 °C over 8 hours, showing no evidence of arene exchange reactions.

The double-sandwich bimetallic nature of complex **2** was confirmed by single-crystal X-ray diffraction. As shown in Fig. 2, each Th center is coordinated with one η^5-Cp^{Ar5} ligand, one reduced aryl ring of the Cp^{Ar5} ligand in an η^6 fashion, and two bridging hydrido ligands. The bridging hydrido ligand (H1) was located using difference Fourier syntheses and refined isotropically. The Th–H distances of 2.26(4) and 2.28(4) Å fall in the range (1.96(3)–2.508(4) Å) found in the previously reported molecular thorium hydride complexes.[8,10]

The coordinated aryl ring (C15–C20) is bent at an angle of only 15.1° relative to the central cyclopentadienyl ring, while the other four aryl rings exhibit an average inclined angle of 63.3°. Unlike the planar symmetric coordination observed in [(Cp^{Ar5})La(μ-H)]$_2$,[9c] the six carbon atoms (C15–C20) adopt a puckered arrangement, indicative of significant 1,4-cyclohexadiene character.[11] The fold angle between the planes defined by the C15 and C18 atoms in the aryl ring is determined to be 16.9°, which indicates the sp^3-character of C15 and C18. Accordingly, two of the Th–C bonds (Th1^i–C15 2.671(6) Å; Th1^i–C18 2.584(6) Å) are shorter when compared to the average value (2.773 Å) for the other four carbon atoms. Furthermore, the C–C bonds of the coordinated aryl ring vary, with C16–C17 (1.379(9) Å) and C19–C20 (1.362(9) Å) being shorter than the other four C–C bonds (1.417(9)–1.460(9) Å). This coordination pattern is comparable

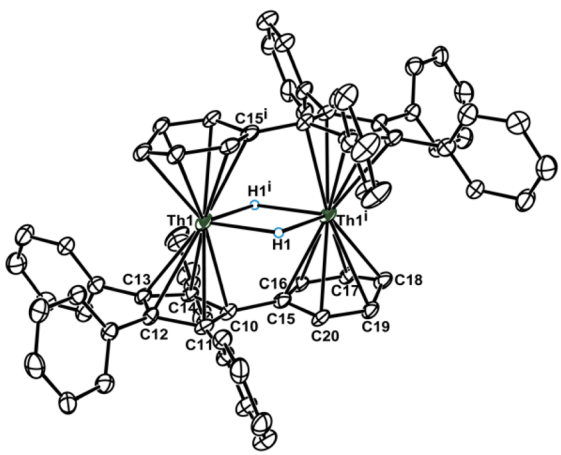

Fig. 2 Molecular structure of complex **2**. All the ^{i}Pr groups and the hydrogen atoms, except the bridging hydrides (H1 and H1^i), are omitted for clarity.

to that of the reported thorium arene complex [{(Et_8-calix[4]tetrapyrrole)Th}{K(DME)}(η^4-$C_{10}H_8$)][Li(DME)$_3$],[4a] where the Th center binds to one ring of the naphthalene in an η^4-manner.

The most notable structural feature of complex **2** is the ultra-short Th⋯Th distance of 3.3617(5) Å. This value is comparable to Th⋯Th distances estimated from twice the thorium metallic radius (3.59 Å, CN = 12)[12] and single-bond radius (3.444 Å).[13] To the best of our knowledge, this is the shortest Th⋯Th distance yet seen in a discrete molecular complex, and significantly shorter than those in complexes [(Cp″)$_2$Th(μ-H)$_3$Th(H)(Cp″)$_2$][K(18-crown-6)(Et$_2$O)] (3.6622(1) Å) (Cp″ = $C_5H_3(SiMe_3)_2$),[10c] [$Me_2Si(C_5Me_4)_2$Th(μ-H)$_2$]$_2$ (3.632(2) Å),[10e] and [(2,6-^{t}Bu$_2$–$C_6H_3O)_2$Th(μ-H)$_2$]$_3$ (3.588(1)–3.818(1) Å).[10i] The relatively short Th⋯Th distance is mainly attributed to the two reduced pentaarylcyclopentadienyl ligands and bridging hydrides, which draw the thorium centers closer together.

Based on the NMR data and crystallographic information, the thorium metal centers should be assigned to tetra-valent states. Meanwhile, the EPR spectrum of complex **2** is silent at 77 K (Fig. S25).

In order to thoroughly comprehend the bonding nature of complex **2**, we performed DFT investigations at the B3PW91 level on the whole molecule. For the thorium atom, a small core pseudopotential and its associated basis set were chosen, in which the f-electrons are included in the valence shell. DFT calculations predict that the ground state of complex **2** is a singlet state, lower by 9.8 kcal mol^{-1} in energy than the triplet state. As depicted in Fig. 3, the HOMO reflects the Th–aryl and Th–Cp ring interactions, and the composition mainly consists of a 25.6% contribution from Th (15.4% 5f and 10.2% 6d), 36.8% from the aryl groups (C15–20 and C15^i–20^i), and 22.2% from the 2p orbitals of the Cp carbon atoms. Similar orbital contributions are also evident in the HOMO−1 orbital. The WBI values (Table S7) of Th–C_{Aryl} (C15–20) range from 0.20 to 0.47. Notably, the WBI values for Th–C15 (0.37) and Th–C18 (0.47) are larger than those for the others (0.20–0.25). NBO analysis reveals the presence of two sigma Th–aryl bonds, Th–C15 (resp. C15^i) and Th–C18 (resp. C18^i), which are strongly polarized toward the carbon atoms (80%). These bonds involve a hybrid sp orbital on the carbon atom (92% 2p and 8% 2s) and a hybrid pdf orbital on the Th atom (81% 6d, 17% 5f and 2% 6p). The existence of these two bonds provides evidence for the formation of the boat-form of a 1,4-hexadienyl anion. The anion formation is further supported by the large WBI values (1.53 in both cases) of the C16–C17 and C19–C20 bonds in aryl ring when compared to the other four bonds (1.06–1.11), as well as the negative charge (Table S8) located on the C18 (−0.55). Thus, the orbital analysis, WBI values, and the average C–C distance of 1.436 Å suggest that the 1,4-cyclohexadienyl, as a dianion, interacts with the Th center through a σ-bond, and the 5f orbitals are critical for stabilizing the aryl ring. The WBI value of Th1–Th1^i is 1.00, indicating the presence of a strong binding interaction between the Th1 and Th1^i, which involves the 6d electrons. Mostly, the Th–Th interaction is found at the second perturbation theory of NBO and indicates donation from Th 6d into the 6d of the other thorium.

The reaction chemistry of complex **2** is fascinating due to the involvement of metal-hydride ligands and tri-anionic pentaarylcyclopentadienyl, which makes it an excellent reductant capable of achieving multi-electron reduction reactivity. As shown in Scheme 2, complex **2** can easily reduce 3 equivalents of tellurium in benzene/THF through a six-electron reduction process to afford [(Cp^{Ar5})Th(THF)]$_2$(μ-Te)$_3$ (**3**) as a red-brown solid in 92% isolated yield. The six-electron reduction can be formally accounted for as two one-electron hydride reductions, generating H_2, and two two-electron (Cp^{Ar5})$^{3-}$-based reductions, yielding the typically monoanionic (Cp^{Ar5})$^-$ ligand. Single crystals of **3** were grown from THF/hexane. As drawn in Fig. 4, the two Th atoms are bridged by three Te^{2-} ligands, and each Th atom is also bonded to an η^5-Cp^{Ar5} ligand and a THF molecule. The Th_2Te_3 core adopts a slightly distorted triangular

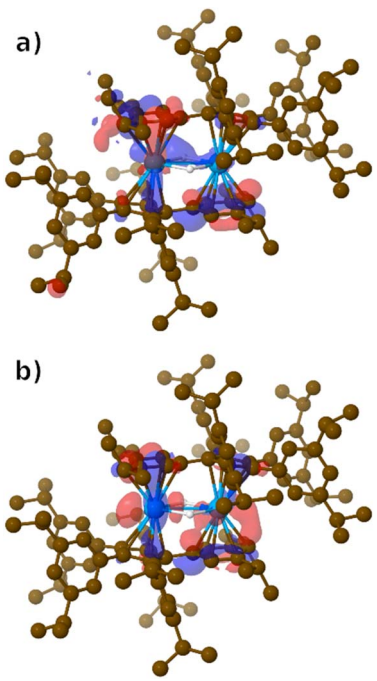

Fig. 3 DFT calculations of complex **2**. (a) HOMO (506, −3.23 eV, isovalue = 0.03) of complex **2**; (b) HOMO − 1 (505, −4.07 eV) of complex **2**. The hydrogen atoms are omitted for clarity.

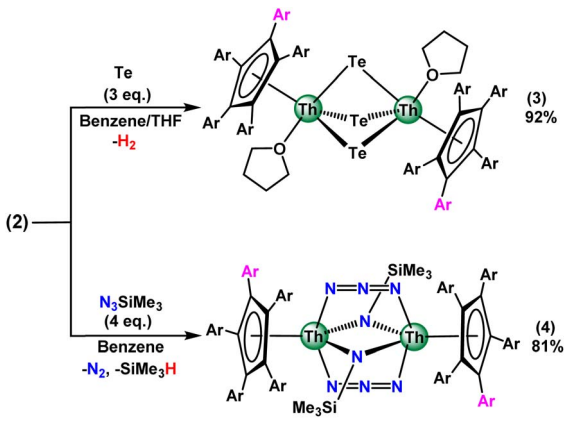

Scheme 2 Reactions of complex **2** with Te and N_3SiMe_3.

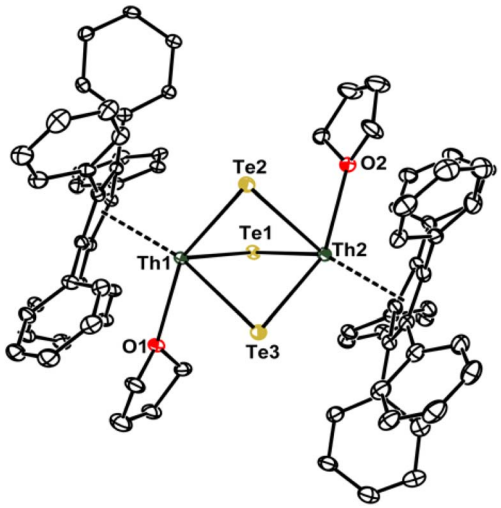

Fig. 4 Molecular structure of complex **3**. All the ^{i}Pr groups and the hydrogen atoms are omitted for clarity.

bipyramid geometry, with the three Te atoms occupying the equatorial positions and the two Th atoms in the apical sites. The Th–Te bond lengths vary from 2.9965(4) to 3.1277(4) Å, which are comparable to the μ_2-bridging U(IV)–Te bond distances found in complex $[\{(SiMe_3)_2N\}_3U]_2(\mu\text{-Te})$ (2.9914(5)–3.0420(5) Å),[14] because of the similar ionic radii of Th^{4+} (1.08 Å) and U^{4+} (1.03 Å).[15]

Complex **2** can also function as a six-electron reductant in the reduction of 4 equivalents of trimethylsilylazide (N_3SiMe_3) in benzene to give $[(Cp^{Ar5})Th(\mu\text{-}N_3)(\mu\text{-}NSiMe_3)]_2$ (**4**) as a pale blue solid in 81% isolated yield. In this case, a distinct color change from dark purple to pale blue was observed, accompanied by the evolution of gas, as evidenced by the bubbling of the solution. In the ^{1}H NMR spectrum, integration of the signals reveals a 1 : 1 ratio between the $SiMe_3$ group and Cp^{Ar5} ligand. As shown in Fig. 5, it lies on a center of inversion, and the asymmetric unit contains a half-dimer. The Th center is coordinated with one η^5-Cp^{Ar5} ligand, two bridging azide (N_3^-) moieties and two bridging imido ($[NSiMe_3]^{2-}$) units. In this transformation, the cleavage of the N=N double bond and N–Si single bond of N_3SiMe_3 occurs simultaneously, releasing N_2 and $SiMe_3H$ without the formation of Me_3Si–$SiMe_3$ (see Fig. S16 and S17). This result is different from the reactions of $[\{(Et_8\text{-calix[4]tetrapyrrole})Th\}\{K(DME)\}(\eta^4\text{-}C_{10}H_8)][Li(DME)_3]$ and $[(Cp^*)_2\text{-}Th(bipy)]$ with N_3SiMe_3, which likely proceed through a thorium-imido intermediate with the transfer of $SiMe_3$ groups to give $[(Et_8\text{-calix[4]tetrapyrrole})Th\{N(SiMe_3)_2\}][Li(DME)_3]$[14a] and $[(Cp^*)_2Th(N_3)\{N(SiMe_3)_2\}]$,[16] respectively (Scheme 2).

Reaction of complex **2** with 3 equivalents of CS_2 gave a thorium trithiocarbonate/dithiolene/sulfide bridged complex $[(Cp^{Ar5})Th(\mu\text{-}\eta^2\text{:}\eta^2\text{-}CS_3)(\mu\text{-}S)(\mu\text{-}\eta^4\text{:}\eta^1\text{-}SCH{=}CHS)Th(Cp^{Ar5})]$ (**5**) as a red-brown solid in 46% isolated yield. X-ray crystallographic studies disclosed the geometry of complex **5** with *cis*-ethenedithiolate, sulfide and trithiocarbonate ligands (Fig. 6). The *cis*-ethenedithiolate ligand, including the C1, C2, S1 and S2 atoms, is almost planar with a maximum deviation of 0.015 Å, and bonds to the Th1 center with η^4-interactions and coordinates to the Th2 center by one S atom (S2) in a μ-pattern. The C1–C2 bond distance (1.36(2) Å) in the dithiolate group matches well with the corresponding bond metrics in $Cp'ReCl_2(SCH{=}CHS)$ (1.343(6) Å, $Cp' = C_5EtMe_4$)[17] and (Bipy)Pt(SCH=CHS) (1.346(14) Å),[18] suggestive of double-bond character. Statistically, the three C–S bond distances of the CS_3^{2-} fragment are very close (1.683(16)–1.748(16) Å), indicating negative charge delocalization. The average C–S bond distance of 1.720(16) Å is comparable to those found in $\{[(Cp^*)_2Th]_2(\mu\text{-}CS_3)_2\}$ (1.707(4) Å)[16] and $\{[\eta^5\text{-}1,3\text{-}(Me_3C)_2C_5H_3]_2Th(\mu\text{-}CS_3)\}_2$ (1.708(2) Å).[20] For the bridging sulfide unit, the Th–S bond distances of 2.767(3) Å and 2.649(3) Å are similar to those observed in $\{[\eta^5\text{-}1,2,4\text{-}(Me_3C)_3C_5H_2]_2Th(\mu\text{-}S)\}_2$ (2.707(2)–2.726(2) Å)[20] and $\{[\eta^5\text{-}1,3\text{-}(Me_3C)_2C_5H_3]_2\text{-}Th(\mu\text{-}S)\}_2$ (2.6684(14) Å and 2.6678(12) Å).[19]

In this reaction, the two $(Cp^{Ar5})^{3-}$ ligands promote the four-electron reduction and cleave the C=S bond of two equivalents of CS_2 to form two equivalents of sulfide (S^{2-}) and carbon monosulfide (CS), respectively (Scheme 3). One of the two sulfides (S^{2-}) reacts with another equivalent of CS_2 to generate trithiocarbonate

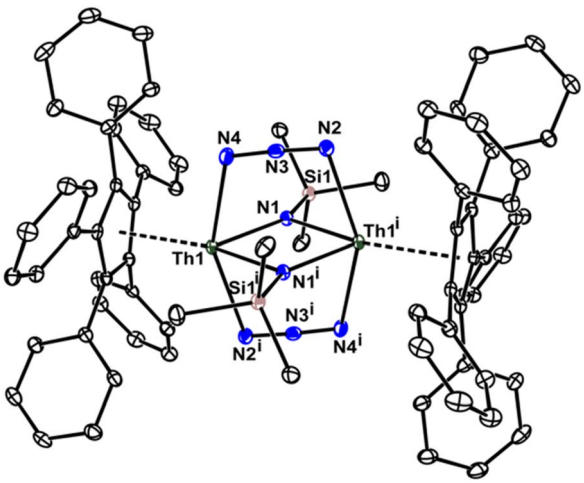

Fig. 5 Molecular structure of complex **4**. All the ^{i}Pr groups and the hydrogen atoms are omitted for clarity.

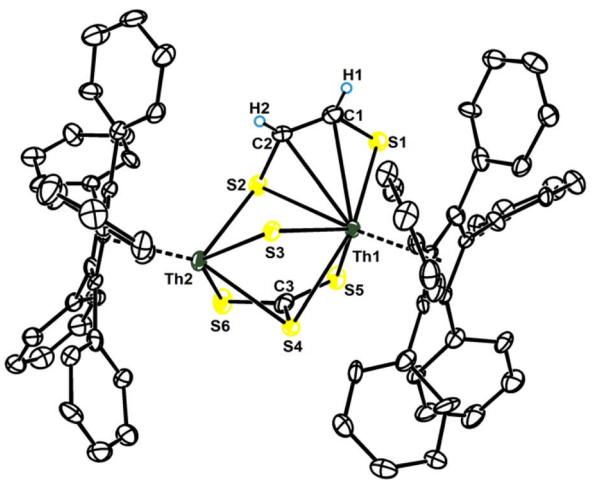

Fig. 6 Molecular structure of complex **5**. All the ^{i}Pr groups and the hydrogen atoms, except H1 and H2 atoms, are omitted for clarity.

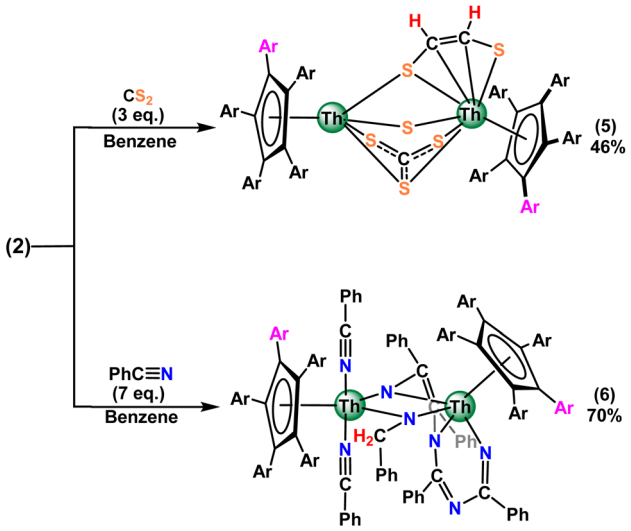

Scheme 3 Reactions of complex **2** with CS_2 and benzonitrile.

(CS_3^{2-}). The two CS units insert into the Th–H bonds and couple to form a dianionic *cis*-ethenedithiolate ($[SCH{=}CHS]^{2-}$) ligand. To the best of our knowledge, this is the first example of a *cis*-ethenedithiolate complex resulting from reductive cleavage of CS_2, mediated by f-elemental metal hydrides.

Treatment of complex **2** with 7 equivalents of benzonitrile in benzene at room temperature afforded a thorium mixed imido/metallacyclic complex $[(Cp^{Ar5})Th(PhCN)_2(\mu\text{-}NCH_2Ph)\{\eta^1,\kappa^3\text{-}NC(Ph){=}C(Ph)NC(Ph){=}NC(Ph){=}N\}Th(Cp^{Ar5})]$ (**6**) as a red-brown crystalline solid in 70% isolated yield. The molecular structure of complex **6** is highlighted in Fig. 7. The imido group (μ_2-NCH_2Ph) symmetrically bridges two Th centers. Four PhCN units are linearly connected in the NCCNCNCN order through the coupling of one C–C bond and two C–N bonds. This chain bonds to the Th1 center through three N atoms in a κ^3-fashion, resulting in the formation of fused five- and six-membered chelate rings, and coordinates to the Th2 center by one N atom in an η^1-pattern. The C–C and C–N bond distances in this chain fall in the standard values of single and double bonds, indicating a partial delocalization of the unit (Fig. S31). Furthermore, two benzonitrile molecules are bound to the Th2 center to fulfill the same coordination number as the Th1 center.

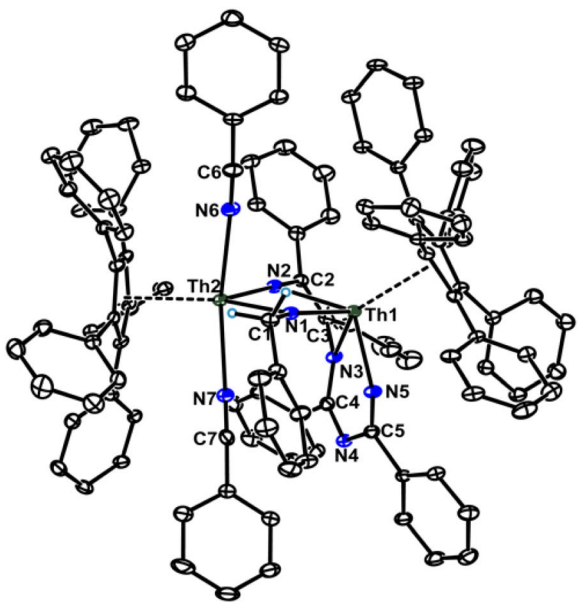

Fig. 7 Molecular structure of complex **6**. All the ^{i}Pr groups and the hydrogen atoms are omitted for clarity.

This reaction involves the double Th–H addition to the C≡N triple bond of one nitrile and a four-electron reductive coupling of four equivalents of nitriles. This transformation is in stark contrast to what was observed previously in either the reaction of $[(Cp^*)_2ThH_2]_2$ with 3 equivalents of $CH_3C{\equiv}N$, which yielded a cyanopentadienyl dianion $[C_6N_3H_7]^{2-}$ through the combination of reduction, insertion, deprotonation and rearrangement,[21] or the reaction of $[(Cp')LuH_2]_4$ ($Cp' = C_5Me_4SiMe_3$) with 10 equivalents of PhC≡N, which gave a linear tetrameric chain $[Ph_4C_4N_4H_2]^{2-}$ in the sequence of CNCNCNCN, accompanied by hydride insertion.[22]

Conclusion

In summary, we have demonstrated for the first time that the penta-arylcyclopentadienyl has a redox-active nature, can serve as not only a typical monoanionic ligand, but also a tri-anionic ancillary ligand to draw two Th atoms in close proximity to form the double-sandwich bimetallic complex. Complex **2** is proposed to form from the selective reduction of one of the five aryl groups of Cp^{Ar5} to a dianionic 1,4-cyclohexadienyl, mediated by transient thorium hydride complex "$[(Cp^{Ar5})ThH_3]_2$" resulting from the hydrogenolysis reaction of the corresponding tri-benzyl precursor. The electrons stored in the hydridic ligands and reduced dianionic 1,4-cyclohexadienyl groups promote the reduction of small molecules by a thorium complex. Complex **2** can be regarded as a Th(II)–H synthon, exhibiting six-electron reduction reactivities toward substrates, such as elemental tellurium and trimethylsilylazide, to afford three Te^{2-} bridged and two mixed azide/imido bridged thorium complexes **3** and **4**, respectively, without undergoing ligand scrambling or ligand loss. Additionally, complex **2** facilitates the reductive coupling of CS_2 and linear quadruple coupling of benzonitrile, concomitant with Th–H addition, to give unique thorium complexes **5** and **6**. Currently, the reactivity of complex **2** toward other substrates is under investigation.

Author contributions

X. S. and G. Q. carried out the synthesis and characterization of complexes **1**–**6**. P. D. assisted in the NMR spectroscopy experiment. I. D. R. and L. M. performed the theoretical calculations. J. C. conceived this project and provided guidance. The manuscript was written through contributions of all authors.

Conflicts of interest

The authors declare no conflict of interest.

Data availability

All data (experimental details, spectroscopic characterization and computational data) that support the findings of this study are available within the article and its SI. See DOI: **https://doi.org/10.1039/d5sc03403e**.

CCDC 1912745 (**1**), 1912746 (**2**), 2106657 (**3**), 2106658 (**4**), 2106659 (**5**) and 2106660 (**6**) contain the supplementary crystallographic data for this paper.[23–28]

Acknowledgements

This work was supported by the National Natural Science Foundation of China (No. 22271272). L. M. is a senior member of the Institut Universitaire de France. The Chinese Academy of Sciences is acknowledged for financial support (LM) and CalMip for a generous grant of computing time.

Notes and references

1 (*a*) F. Ortu, A. Formanuik, J. R. Innes and D. P. Mills, *Dalton Trans.*, 2016, **45**, 7537; (*b*) S. T. Liddle, *Coord. Chem. Rev.*, 2015, **293**, 211.

2 (*a*) R. R. Langeslay, M. E. Fieser, J. W. Ziller, F. Furche and W. J. Evans, *Chem. Sci.*, 2015, **6**, 517; (*b*) J. C. Wedal, J. M. Barlow, J. W. Ziller and J. Y. Yang, *Chem. Sci.*, 2021, **12**, 8501; (*c*) J. Q. Nguyen, L. M. Anderson-Sanchez, W. N. G. Moore, J. W. Ziller, F. Furche and W. J. Evans, *Organometallics*, 2023, **42**, 2927.

3 (*a*) P. C. Blake, M. F. Lappert, J. L. Atwood and H. Zhang, *J. Chem. Soc. Chem. Commun.*, 1986, **15**, 1148; (*b*) D. N. Huh, S. Roy, J. W. Ziller, F. Furche and W. J. Evans, *J. Am. Chem. Soc.*, 2019, **141**, 12458; (*c*) P. C. Blake, N. M. Edelstein, P. B. Hitchcock, W. K. Kot, M. F. Lappert, G. V. Shalimoff and S. Tian, *J. Organomet. Chem.*, 2001, **636**, 124; (*d*) R. R. Langeslay, M. E. Fieser, J. W. Ziller, F. Furche and W. J. Evans, *J. Am. Chem. Soc.*, 2016, **138**, 4036; (*e*) R. R. Langeslay, G. P. Chen, C. J. Windorff, A. K. Chan, J. W. Ziller, F. Furche and W. J. Evans, *J. Am. Chem. Soc.*, 2017, **139**, 3387; (*f*) J. S. Parry, F. G. N. Cloke, S. J. Coles and M. B. Hursthouse, *J. Am. Chem. Soc.*, 1999, **121**, 6867; (*g*) J. R. Walensky, R. L. Martin, J. W. Ziller and W. J. Evans, *Inorg. Chem.*, 2010, **49**, 10007; (*h*) N. A. Siladke, C. L. Webster, J. R. Walensky, M. K. Takase, J. W. Ziller, D. J. Grant, L. Gagliardi and W. J. Evans, *Organometallics*, 2013, **32**, 6522; (*i*) A. B. Altman, A. C. Brown, G. Rao, T. D. Lohrey, R. D. Britt, L. Maron, S. G. Minasian, D. K. Shuh and J. Arnold, *Chem. Sci.*, 2018, **9**, 4317; (*j*) A. Formanuik, A. M. Ariciu, F. Ortu, R. Beekmeyer, A. Kerridge, F. Tuna, E. J. L. McInnes and D. P. Mills, *Nat. Chem.*, 2017, **9**, 578; (*k*) J. T. Boronski, J. A. Seed, D. Hunger, A. W. Woodward, J. van Slageren, A. J. Wooles, L. S. Natrajan, N. Kaltsoyannis and S. T. Liddle, *Nature*, 2021, **598**, 72; (*l*) J. Q. Nguyen, J. C. Wedal, J. W. Ziller, F. Furche and W. J. Evans, *Inorg. Chem.*, 2024, **63**, 6217.

4 (*a*) I. Korobkov, S. Gambarotta and G. P. A. Yap, *Angew. Chem., Int. Ed.*, 2003, **42**, 814; (*b*) I. Korobkov, S. Gambarotta and G. P. A. Yap, *Angew. Chem., Int. Ed.*, 2003, **42**, 4958; (*c*) I. Korobkov and S. Gambarotta, *Organometallics*, 2004, **23**, 5379; (*d*) F.-C. Hsueh, D. Chen, T. Rajeshkumar, R. Scopelitti, L. Maron and M. Mazzanti, *Angew. Chem., Int. Ed.*, 2024, **63**, e202317346; (*e*) F.-C. Hsueh, T. Rajeshkumar, B. Kooij, R. Scopelitti, K. Severin, L. Maron, I. Zivkovic and M. Mazzanti, *Angew. Chem., Int. Ed.*, 2023, **62**, e202215846; (*f*) C. Yu, J. Liang, C. Deng, G. Lefèvre, T. Cantat, P. L. Diaconescu and W. Huang, *J. Am. Chem. Soc.*, 2020, **142**, 21292; (*g*) L. M. Anderson-Sanchez, A. Rajabi, J. C. Wedal, J. W. Ziller, F. Furche and W. J. Evans, *Organometallics*, 2024, **43**, 2027.

5 (*a*) H. S. La Pierre and K. Meyer, *Prog. Inorg. Chem.*, 2014, **58**, 303; (*b*) M. Ephritikhine, *Organometallics*, 2013, **32**, 2464; (*c*) M. Sharma and M. S. Eisen, *Struct. Bonding*, 2008, **127**, 1; (*d*) F. T. Edelmann, in *Complexes of actinide elements in Comprehensive Organometallic Chemistry III*, ed. R. H. Crabtree and D. M. P. Mingos, Elsevier, Oxford, 2007, vol. 4.02, pp. 191–242; (*e*) T. Shima and M. Hou, *Recent Development in Clusters of Rare Earths and Actinides: Chemistry and Materials*, 2017, vol. 173, pp. 315–335; (*f*) W. J. Evans, K. A. Miller, S. A. Kozimor, J. W. Ziller, A. G. DiPasquale and A. L. Rheingold, *Organometallics*, 2007, **26**, 3568.

6 R. Chen, G. Qin, S. Li, A. J. Edwards, R. O. Piltz, I. D. Rosal, L. Maron, D. Cui and J. Cheng, *Angew. Chem., Int. Ed.*, 2020, **59**, 11250.

7 L. D. Field, C. M. Lindall, A. F. Masters and G. K. B. Clentsmith, *Coord. Chem. Rev.*, 2011, **255**, 1733.

8 G. Qin, Y. Wang, X. Shi, I. D. Rosal, L. Maron and J. Cheng, *Chem. Commun.*, 2019, **55**, 8560.

9 (*a*) X. Shi, G. Qin, Y. Wang, L. Zhao, Z. Liu and J. Cheng, *Angew. Chem., Int. Ed.*, 2019, **58**, 4356; (*b*) L. Zhao, P. Deng, X. Gong, X. Kang and J. Cheng, *ACS Catal.*, 2022, **12**, 7877; (*c*) X. Shi, P. Deng, T. Rajeshkumar, L. Maron and J. Cheng, *Chem. Sci.*, 2024, **15**, 11965; (*d*) Y. Wang, I. K. Del, G. Qin, L. Zhao, L. Maron, X. Shi and J. Cheng, *Chem. Commun.*, 2021, **57**, 7766.

10 (*a*) R. W. Broach, A. J. Schultz, J. M. Williams, G. M. Brown, J. M. Manriquez, P. J. Fagan and T. J. Marks, *Science*, 1979, **203**, 172; (*b*) P. J. Fagan, J. M. Manriquez, E. A. Maatta, A. M. Seyam and T. J. Marks, *J. Am. Chem. Soc.*, 1981, **103**, 6650; (*c*) R. R. Langeslay, M. E. Fieser, J. W. Ziller, F. Furche and W. J. Evans, *J. Am. Chem. Soc.*, 2016, **138**, 4036; (*d*) W. Ren, E. Zhou, B. Fang, G. Zi, D.-C. Fang and M. D. Walter, *Chem. Sci.*, 2014, **5**, 3165; (*e*) C. M. Fendrick, L. D. Schertz, V. W. Day and T. J. Marks, *Organometallics*, 1988, **7**, 1828; (*f*) W. Ren, N. Zhao, L. Chen, H. Song and G. Zi, *Inorg. Chem. Commun.*, 2011, **14**, 1838; (*g*) E. Zhou, W. Ren, G. Hou, G. Zi, D.-C. Fang and M. D. Walter, *Organometallics*, 2015, **34**, 3637; (*h*) W. J. Evans, G. W. Nyce and J. W. Ziller, *Organometallics*, 2001, **20**, 5489; (*i*) D. L. Clark, S. K. Grumbine, B. L. Scott and J. G. Watkin, *Organometallics*, 1996, **15**, 949; (*j*) A. B. Altman, A. C. Brown, G. Rao, T. D. Lohrey, R. D. Britt, L. Maron, S. G. Minasian, D. K. Shuh and J. Arnold, *Chem. Sci.*, 2018, **9**, 4317.

11 (*a*) W. J. Evans, S. A. Kozimor, J. W. Ziller and N. Kaltsoyannis, *J. Am. Chem. Soc.*, 2004, **126**, 14533; (*b*) W. J. Evans, C. A. Traina and J. W. Ziller, *J. Am. Chem. Soc.*, 2009, **131**, 17473; (*c*) C. M. Kotyk, M. E. Fieser, C. T. Palumbo, J. W. Ziller, L. E. Darago, J. R. Long, F. Furche and W. J. Evans, *Chem. Sci.*, 2015, **6**, 7267; (*d*) T. W. Graham, J. Kickham, S. Courtenay, P. Wei and D. W. Stephan, *Organometallics*, 2004, **23**, 3309; (*e*) J. N. Boynton, J.-D. Guo, F. Grandjean, J. C. Fettinger, S. Nagase, G. J. Long and P. P. Powder, *Inorg. Chem.*, 2013, **52**, 14216.
12 P. Pyykkö, *J. Phys. Chem. A*, 2015, **119**, 2326.
13 L. Pauling and B. Kamb, *Proc. Natl. Acad. Sci. U. S. A.*, 1986, **83**, 3569.
14 J. L. Brown, G. Wu and T. W. Hayton, *Organometallics*, 2012, **32**, 1193.
15 R. D. Shannon, *Acta Crystallogr., Sect. A*, 1976, **32**, 751.
16 P. Yang, E. Zhou, B. Fang, G. Hou, G. Zi and M. D. Walter, *Organometallics*, 2016, **35**, 2129.
17 J. A. Kanney, B. C. Noll and M. R. DuBois, *J. Am. Chem. Soc.*, 2002, **124**, 9878.
18 C. E. Keefer, R. D. Bereman, S. T. Purrington, B. W. Knight and P. D. Boyle, *Inorg. Chem.*, 1999, **38**, 2294.
19 W. Ren, H. Song, G. Zi and M. D. Walter, *Dalton Trans.*, 2012, **41**, 5965.
20 W. Ren, G. Zi, D.-C. Fang and M. D. Walter, *J. Am. Chem. Soc.*, 2011, **133**, 13183.
21 W. J. Evans, K. A. Miller and J. W. Ziller, *Angew. Chem., Int. Ed.*, 2008, **47**, 589.
22 D. Cui, M. Nishiura and Z. Hou, *Angew. Chem., Int. Ed.*, 2005, **44**, 959.
23 X. Shi, G. Qin, P. Deng, I. Del Rosal, L. Maron and J. Cheng, CCDC 1912745: Experimental Crystal Structure Determination, 2025, DOI: **10.5517/ccdc.csd.cc226cg4**.
24 X. Shi, G. Qin, P. Deng, I. Del Rosal, L. Maron and J. Cheng, CCDC 1912746: Experimental Crystal Structure Determination, 2025, DOI: **10.5517/ccdc.csd.cc226ch5**.
25 X. Shi, G. Qin, P. Deng, I. Del Rosal, L. Maron and J. Cheng, CCDC 2106657: Experimental Crystal Structure Determination, 2025, DOI: **10.5517/ccdc.csd.cc28q4pv**.
26 X. Shi, G. Qin, P. Deng, I. Del Rosal, L. Maron and J. Cheng, CCDC 2106658: Experimental Crystal Structure Determination, 2025, DOI: **10.5517/ccdc.csd.cc28q4qw**.
27 X. Shi, G. Qin, P. Deng, I. Del Rosal, L. Maron and J. Cheng, CCDC 2106659: Experimental Crystal Structure Determination, 2025, DOI: **10.5517/ccdc.csd.cc28q4rx**.
28 X. Shi, G. Qin, P. Deng, I. Del Rosal, L. Maron and J. Cheng, CCDC 2106660: Experimental Crystal Structure Determination, 2025, DOI: **10.5517/ccdc.csd.cc28q4sy**.